CALIBRATION OF LANDSAT-8 TIRS BANDS FOR ENVIRONMENT CHANGE DETECTION

D. Caselles[a,*], V. Caselles[a], R. Pérez[b], E. Valor[a], C. Doña[a], V. García-Santos[a], R. Niclòs[a], M.J. Barberá[a], J.M. Sánchez[c], C. Coll[a], J.A. Valiente[d]

[a]Departamento de Física de la Tierra y Termodinámica, Universidad de Valencia, Doctor Moliner 50, 46100 Burjassot (Valencia), Spain.
[b]Departamento de Ingeniería Química y Nuclear, Universidad Politécnica de Valencia, Camino de Vera s/n, 46022 Valencia, Spain.
[c]Departamento de Física Aplicada, Universidad de Castilla-La Mancha, Plaza Manuel Meca 1, 13400 Almadén (Ciudad Real), Spain.
[d]Instituto Universitario Centro de Estudios Ambientales del Mediterraneo, Charles Darwin 14, 46980 Paterna (Valencia), Spain.

THEME: Airborne and Innovative Remote Sensing Platforms and Techniques

KEY WORDS: Calibration, Landsat-8, TIRS Bands, Environment Changes

ABSTRACT:

The Landsat-8 (L8) was launched on February 2013, and operational acquisitions started middle April 2013. The L8 Thermal Infrared Sensor (TIRS) has two thermal bands, 10 (11.60-11.19 µm) and 11 (11.50-12.51), aimed to provide more accurate Land Surface Temperature (LST) than the Landsat-7ETM+, at 100-m spatial resolution. The first studies by the L8 calibration team showed TIRS temperature offsets, and in January 2014 they proposed subtracting 2.1 ± 0.8 K and 4.4 ± 1.8 K from temperatures measured by band 10 and 11. The aim of this study is to contribute to the TIRS calibatrion efforts with the objective to solve the current problems in order to can use L8 in environment change detection.

Ground transects measurements of LST performed in a 100 km^2, flat and thermally homogeneous area of rice-crop fields (39.295ºN, -0.308ºE in WGS-84, at sea level) close to Valencia-Spain, were used for the vicarious calibration of the L8 thermal bands. Three different surface conditions were covered during the measurement period: flooded soil (water surface), bare soil and rice with full vegetation cover, with LSTs ranging from less than 10ºC to 30ºC. Four TIR radiometers were used to perform the transects: two CIMEL CE 312-1 with four bands (8-13, 11.5-12.5, 10.5-11.5 and 8.2-9.2 µm) and two CIMEL 312-2 with six (8-13, 8.1-8.5, 8.5-8.9, 8.9-9.3, 10.3-11.0 and 11.0-11.7 µm). Calibration against a reference blackbody ensured absolute accuracy of all the radiometer bands within 0.1-0.2 K. The CE 312 radiometers were carried back and forth along transects of 100 m in length, and temperatures measured within 3 min centred at the satellite overpass time were averaged. Field emissivity measurements were also performed.

Significant differences between *in situ* and L8 temperatures were observed, and the recalibration proposed by the L8 team was shown not to be satisfactory.

INTRODUCTION

Since the first satellite of Earth observation with thermal channels, the HCMM (Heat Capacity Mapping Mission), were measured uncalibrated various degrees in all of them [1]. Our group is part of the research teams conducting field experiments designed to gauge the satellites. To do this, use the area of rice fields surrounding the Albufera of Valencia and for several years have calibrated the satellite AATSR (Advanced Along-Track Scanning Radiometer) of ESA and MODIS (Moderate Resolution Imaging Spectroradiometer), ASTER (Advanced Spaceborne Thermal Emission and Reflection Radiometer) and Landsat-7 / ETM + (Enhanced Thematic Mapper) NASA [2-6]. Currently, we are conducting an experimental campaign for the calibration of Landsat-8 since the first studies of equipment calibration temperatures showed that satellite unbalanced as revealed NASA in January 2014 (http://landsat.usgs.gov/calibration_notices.php).

The aim of this paper is to contribute to studies being undertaken to calibrate thermal satellite channels L8.

METHODOLOGY

The calibration source black body: a portable source of high accuracy and variable temperature, designed to operate at temperatures from -10 to 80 ° C (Figure 2). Table 2 shows the technical specifications. For more details see [7]. This source of black body participated in a comparison of IR instruments held by the Committee Satellite Earth Observation (CEOS) at the National Physical Laboratory (NPL) in London, against benchmarks [8]. The results showed that the model matched the NPL reference radiometer with an error of ± 0.15 K for temperatures of 20-30 ° C.

Table 2. Specifications of the calibration source [7].

Maximum working temperature	**80 ºC (175 ºF)**
Temperature range	-10 a 80ºC (15 a 175 ºF)
Stability	Less than ± 0.5 K stability for a period of 30 minutes
Heating rate	From ambient temperature to 75 ºC: 60 minutes
Cooling rate	20 a -10 ºC: 90 min (depends on the environment)
Radiation cavity	Material: aluminum blackened Design: conical 120º Inner Diameter: 50 mm Internal length: 155 mm
Emissivity	>0,995
Power consumption	0,2 kW (220/240 V)
Overall Dimensions	Height: 185 mm Width: 260 mm Depth: 315 mm
Weight	Net: 11 kg Gross: 13 kg

Table 3. Specifications of the radiometers used [9].

Input powe	2,5 V
Absolute accuracy	± 0,2 ºC de -10 a 65 ºC ± 0,5 ºC de -40 a 70 ºC
Uniformity	± 0,1 ºC de -10 a 65 ºC ± 0,3 ºC de -40 a 70 ºC
Repeatability	± 0,05 ºC de -10 a 65 ºC ± 0,1 ºC de -40 a 70 ºC
Weight	190 grams
Overall dimensions	6,3 cm de lenght 2,3 cm de diameter
Response time	<1 second to changes in target temperature
Output target temperature	60 µV per ºC
Wavelength range	8 a 14 micrometers
Field of view	22º
Work conditions	-55 a 80ºC 0-100% RH non-condensing Highly water resistant Designed for continuous outdoor use

Figure 2. Source of calibration used..

Figure 3. Radiometer APOGEE SI-211

The radiometer is an infrared temperature sensor that provides a means of contactless measurement of the surface temperature of an object at a certain distance, detecting the infrared radiation emitted by it (Figure 3). Table 3 shows the technical specifications of the radiometer used. For more details see [9].

First, connect together the various devices needed for the measures we are going to make (Figure 4). Then program the calibration source at a temperature of -4 ° C. Then we repeat this procedure until you reach 50 ° C in steps of 5 ° C.

Figure 4. Experimental arrangement for calibration of the radiometer APOGEE SI-211

Spectroradiometer: is an instrument to measure the spectrum emissivity of a surface between 2 and 16 microns (Figure 5). Table 4 shows the technical specifications of spectroradiometer used. For more details see [10].

Table 4. Technical Specifications Spectroradiometer [10].

Spectral Range	2 a 16 micrometers
Spectral resolution	4, 8 y 16 cm^{-1} adjustables Optional: 2 cm^{-1}
Spectral accuracy	+/- 1 cm^{-1} spectral range through
Scanning Speed	1 scan per second
Optical Performance	0,016 cm^2 steradian
Analog to digital converter	16 bits
FFT Size	1024 at 32768
Type of Computer	Compatible PC
Processor/RAM	Pentium 166/128 MB
Hard Drive Capacity	20 GB
Software	Windows 2000™
Operating temperature range	15 to 35 ºC (instrument temperatura)
Overall Size	Length: 35.56 cm Width: 20.32 cm Height: 22.86 cm
Weight	6,8 kg
Power	50 Watts max.

The experimental part we have carried out with the spectroradiometer D & P 102 Win2K model was performed in two different environments. The first part, the calibration of the instrument with his own Black Body, has been done in the laboratory (Figure 5). While the second part of measuring soil samples, was run on an open-air (Figure 7).
To start using the tool, fill the tank of liquid nitrogen to reduce and maintain a 70 K temperature sensor. Then assemble the different parts of Spectroradiometer (Figure 6).

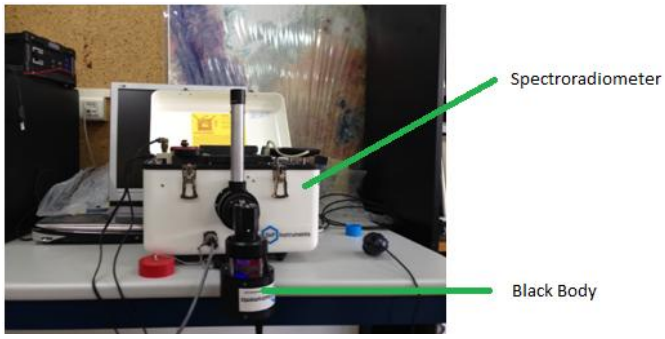

Figure 5. Calibration with Black Body in the laboratory

Figure 6. Spectroradiometer D & P Model 102 Win2K

We set the spectroradiometer on desert sand plaster White Sands in New Mexico, USA This show is already fully characterized and will serve as a reference for checking that both the measures and their subsequent treatment are correct. The second sample we measure is the soil near the Albufera rice fields. This displays is what we have to characterize. Assembly, for both samples, is performed on a tripod for the specific instrument (Figure 7).

The L8 is a satellite of Earth observation, which was launched on February 11, 2013 (Figures 8 and 9). Tables 5 and 6 show the technical specifications of the satellite. For more details see [11].

Figure 7. Mounting the spectroradiometer with sample White Sands (left), with the reflective panel (center) and the paddy soil sample (right).

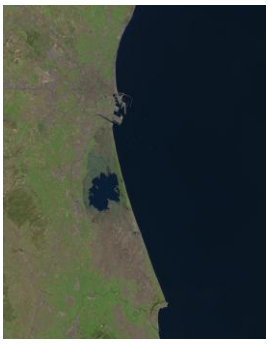

Figure 8. Image Landsat-8.

Figure 9. Satellite Landsat-8

Table 5. Specifications Landsat-8 [11].

Orbit	Sun-synchronous
Orbital Height	705 km
Tilt	98,2º
Crossing Ecuador	At 10:00 (± 15 min) local solar time (descending order)
Viewing width	180 km
Revisit time	16 days
Period of revolution	98,9 minutes
Data Storage	Solid State Data Recorder 3,14 terabits
Data Transmission	X-band, 384 MB
Propulsion	395 kg of monopropellant hydrazine with 8 thrusters of 22 N
Accuracy	0,5 ºC
Weight	2,782 kg
Lifetime	5 years

Table 6. Thermal bands with their respective spectral range and spatial resolution.

Thermal Channels	Spectral Range (micrometers)	Resolution (m)
10	10.6-11.2	100
11	11.5-12.5	100

CIMEL CE 312 is a high precision radiometer to measure the spectral radiance in 4 or 6 thermal infrared bands (Figure 10). These radiometers participated in a comparison of IR instruments held by the Committee Satellite Earth Observation (CEOS) at the National Physical Laboratory (NPL) in London, against benchmarks [12]. The results showed that the model matched the radiometer

radiometer NPL reference within ± 0.2 K for all bands at 20-30 ° C. Table 7 shows the technical specifications of the radiometer used. For more details see [13].

Table 7. Technical Specifications radiometer [13].

MEASURES	Accuract¡y	0,1 ºC
	Resolution	0,01 ºC
	Response Time	1 s
	Repeatability	>99,65%
	IFOV	10º
SENSOR	Type	Silicon Thermopile
	Response Capacity	120 W m^{-2}
	Detectivity	1,6 x10^{8} cm $Hz^{-1/2}$ / W^{-1}
Spectral Channels	Channel W	8 - 14 µm
	Channel N12	11,50 - 12,50 µm
	Channel N11	10,30 - 11,30 µm
	Channel N9	8,20 - 9,20 µm
ENVIRONMENT	Temperature	From -20 to 50 ºC
Size	Cabeza	80 mm in diameter 250 mm in length 1kg weight
	Cable de medida	3 m

Figure 10. CIMEL radiometer CE 312 with built computer.

To obtain in situ data in the area near the Albufera rice fields, we use six APOGEE SI-211, 4 CIMEL CE-312 and the spectroradiometer D & P 102 Win2K model. The ten radiometers are scattered all over the area of measures to cover the maximum area. Each radiometer carried out transects of 100 meters or so. Meanwhile, the fixed espectorradiómetro is placed on the tripod and emissivity measurements are executed. Then transects begin 10 minutes before the time of the satellite pass and finished 10 minutes later. The spectroradiometer also starts measuring at the same time but remains solid. The process of obtaining the temperature measured by the satellite ground begins with obtaining black body temperature satellite radiance from by Planck's law, which describes the electromagnetic radiation emitted by a black body in balance heat at a defined temperature. The intensity of the radiation emitted by a black body or spectral radiance, R (ν, T) [J • m -2 • sr-1], with a certain temperature T [K] and ν frequency [Hz], is given by :

$$R\,(\nu,T) = \frac{2h\nu^3}{c^2}\,\frac{1}{e^{\frac{h\nu}{kT}}-1} \qquad (1)$$

where h is Planck's constant [J • s], c is the speed of light [m / s] k is the Boltzmann constant [J / K]. Then the black body temperature of soil is obtained from the temperature of black body satellite, using atmospheric correction, which involves inserting a sounding of the day and time of satellite overpass a radiative transfer model as the MODTRAN-5 [14]. Finally, to obtain the soil temperature is applied to the black body temperature correction emissivity floor [15]. And the location of a point error is one pixel, the average of a 3x3 matrix is performed pixel.

RESULTS

In the graphs in Figure 12 calibration we've done 3 Apogees SI-211 model is appreciated. Calibration interval going from -4 to 50 ° C. In Figure 13, we see that the radiometer SI-2114 at very low temperatures or very high overestimates the actual value at 1.8 ° C, whereas at temperatures close to ambient, maximum 0.5 ° C about the undervalued . The SI-2118 and IS-2119 radiometer show more accurate measurements than before, producing a maximum overestimation of temperature of 0.3 ° C (0 ° C) and an underestimation

of 0.3 ºC (at -4 ° C).

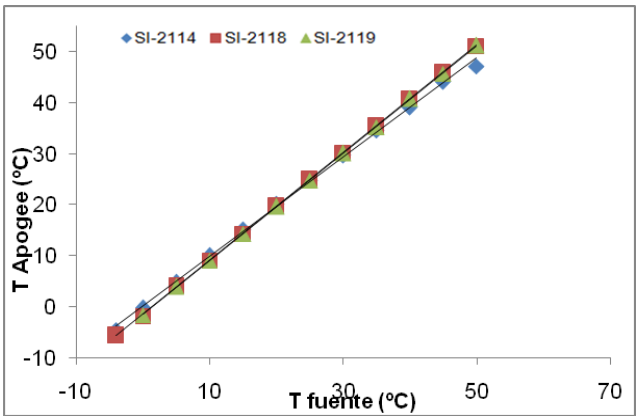

Figure 12. Graph 3 radiometers calibrated APOGEE SI-211

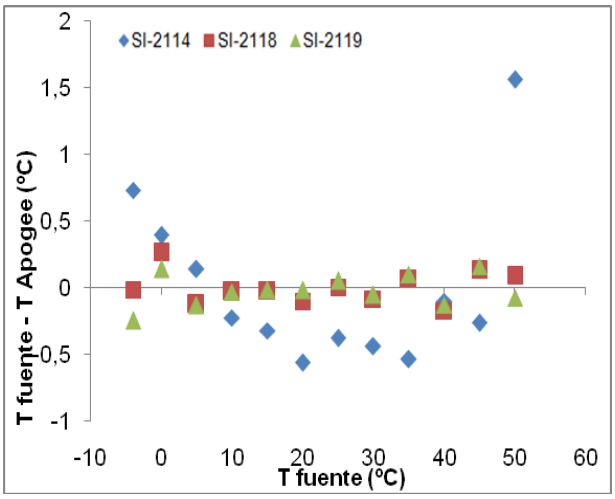

Figure 13. Graph of precision 3 SI-211 APOGEE radiometers calibrated.

In Figure 14 the emissivity coefficients White Sands, both of our measurements (red line) as those of the Aster library (blue line) [16], as a function of wavelength are shown. The characteristic minimum of sands between 8.3 and 9.3 microns, then take the maximum values of emissivity is observed. Furthermore, a large similarity between the graph of our measurements and appreciated Aster. Are also identified areas in which they operate channels 10 (green) and 11 (yellow) of Landsat-8.

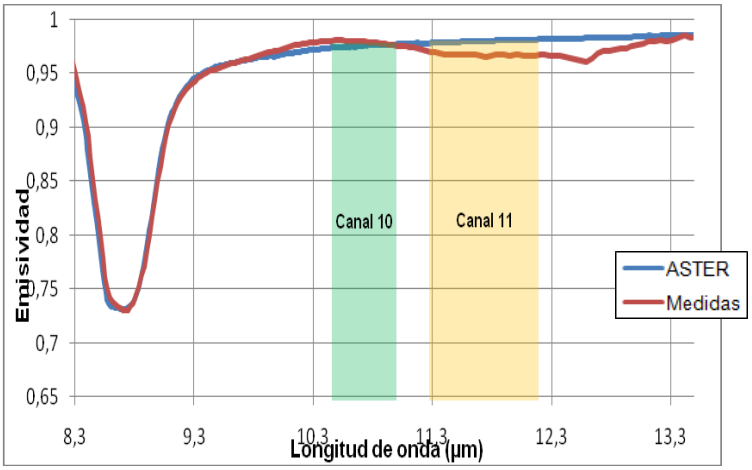

Figure 14. Graph of White Sands emissivity as a function of wavelength

Table 8. Coefficients emissivity of White Sands for channels 10 and 11 of Landsat-8.

	Channel 10	Channel 11
Measures	0,978 ± 0,007	0,968 ± 0,009
ASTER	0,977 ± 0,001	0,981 ± 0,001

Table 9. emissivity values obtained by [17] and our measures to channels 10 and 11 of Landsat-8.

	Channel 10	Channel 11
Measures	0,960 ± 0,005	0,951 ± 0,001
[17]	0,957 ± 0,005	0,954 ± 0,005

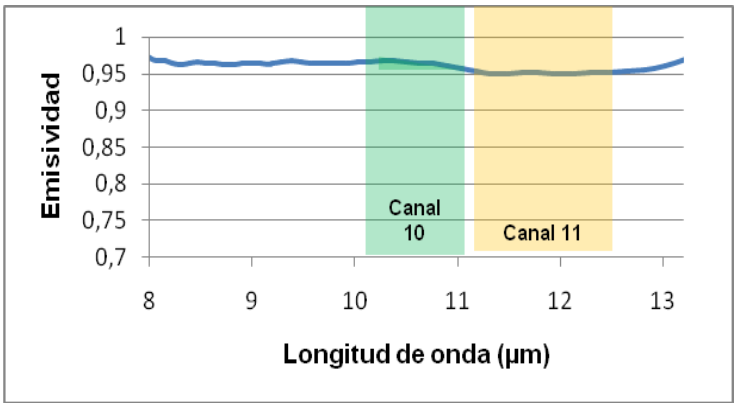

Figure 15. Graph of the paddy soil emissivity as a function of wavelength.

In Figure 15 the emissivity coefficients paddy soil, depending on the wavelength are shown. It is seen that the values between 8 and 13 microns are very similar, just vary between 0.950 and 0.975 microns. Are also identified areas in which they operate channels 10 (green) and 11 (yellow) of Landsat-8.

Emissivity values obtained by [17] and our measures to channels 10 and 11 of Landsat-8 are shown in Table 9. For channel 10 the difference is an overestimation of 3 ms, while for channel 11 the difference is an underestimation of 3 ms.

In Tables 10-13 temperatures obtained through the channels 10 and 11 of Landsat-8, as well as, in situ measurements are observed. In view of these results, we conclude that the channel 10 of L8 presents a calibration error of 2.3 ± 0.9 ° C, while channel 11 has a calibration error of 1.1 ± 1.9 ° C.

Table 10. Temperatures in situ and Landsat-8 for the day January 27, 2014.

		Temperatura (ºC)
LST (*in situ*)		12,0 ± 0,3
Landsat-8	**Channel 10**	14,3 ± 0,9
	Channel 11	15,6 ± 1,9

Table 11. Temperatures in situ and Landsat-8 for the day February 12, 2014.

		Temperatura (ºC)
LST (*in situ*)		12,4 ± 0,6
Landsat-8	**Channel 10**	14,3 ± 0,9
	Channel 11	15,6 ± 1,9

Table 12. Temperatures in situ and Landsat-8 for the day March 16, 2014.

		Temperatura (ºC)
LST (*in situ*)		22,3 ± 1,8
Landsat-8	**Channel 10**	14,3 ± 0,9
	Channel 11	15,6 ± 1,9

Table 13. Temperatures in situ and Landsat-8 on April 10, 2014.

		Temperatura (ºC)
LST (*in situ*)		33 ± 2
Landsat-8	**Channel 10**	14,3 ± 0,9
	Channel 11	15,6 ± 1,9

CONCLUSIONS

1.- We Calibrated radiometers APOGEE 6 SI-211 and have found that errors in temperature measurement range between 0.1 and 0.4 K.

2. We measured soil emissivity of the Albufera rice fields and we have seen that for channel 10 the difference is an overestimation of 3 mils; while for channel 11 the difference is an underestimation of 3 ms.

3. We measured the temperature in the rice fields and we have obtained from images of L8, comparing both we can conclude that the L8 channel 10 has a calibration error of 2.3 ± 0.9 ° C, while channel 11 has a calibration error of 1.1 ± 1.9 ° C.

Acknowledgements: The authors wish to express our gratitude to the Generalitat Valenciana (GVPROMETEOII2014-086 Project) and MINECO (CGL2010-17577-CLI) for the funding received.

References

[1] Caselles, V., Gandia, V., Meliá, J. (1983), Agric. Meteorol .: 30, 77-82.
[2] Coll, C., Caselles, V., Galve, JM, Valor, E., Niclós, R., Sánchez, JM, Rivas, R., (2005, Rem. Sens. Environ .: 97, 288- 300.
[3]. Coll, C., Caselles, V., Galve, JM, Valor, E., Niclós, R., Sánchez, JM, (2006), J. Geophys. Res .: 111, D12105, doi: 10.1029 / 2005JD006830.
[4] Coll, C., Caselles, V., Valor, E., Niclós, R., Sánchez, JM, Galve, JM, Mira, M., (2007), Temperature, Rem. Sens. Environ .: 110, 162-175.
[5] Coll. C., Galve, JM, Sánchez, JM, Caselles, V., (2010), IEEE Trans. Geosc. Rem. Sens .: 48, 547-555.
[6]. Coll, C., Caselles, V., Valor, E., Niclós, R. (2012), Rem. Sens. Environ .: 117, 199-210.
[7]. Theocharous, E., Fox, NP (2010b), NPL REPORT OP4. Teddington, UK.
[8] Land infrared (2001), Landcal Blackbody Source Type P80P Operating Instructions, 13 pp.
[9] Apogee Instruments (2010), SI-211 Precision Infrared Radiometer Instruction Manual, 12 pp.
[10]. D & P Instruments (2006), Model 102 Instruction Manual Portable FTIR, 26 pp.
[11] Rozenstein, O., Qin, Z., Derimian, Y., Karnieli, A. (2014), Sens .: 4, 5768-5780.
[12] Theocharous, E., Usadi, E., Fox, NP (2010a). NPL REPORT OP3. Teddington, UK.
[13] CIMEL Instruments (2014), CE 312: High Precision IR Radiometer Instruction Manual, 6 pp.
[14] García-Santos, V., Valor, E., Caselles, V., Mira, M., Galve, JM, Coll, C. (2013), IEEE Trans. Geos. Rem. Sens .: 51, 2155-2165.
[15] Caselles, V. Martinez, L. (2004), Journal of Remote Sensing 22, 13-18.
[16] Baldridge, AM, Hook, SJ, Grove, CI, Rivera, G. (2009), Rem. Sens. Environ .: 113, 711-715.
[17] Caselles, E., Valor, E., Abad, F., Caselles, V. (2012), Rem. Sens. Environ